

## **Supplementary Information.**

### **Supplementary material and methods**

**Reagents.** Thapsigargin (Tg), Brefeldin (Bref), Tunicamycin (Tm), Cycloheximide (CHX), Puromycin, Propidium Iodide (PI), Polibrene, Bafilomycin (Baf), anti-c-Myc Agarose Affinity Gel antibody, Oligomycin, Carbonyl cyanide-p-trifluoromethoxyphenylhydrazone (FCCP), Rotenone, and Antimycin A were purchased from Sigma-Aldrich. Mitotracker Green, MitoTracker Red CMXRos, Pluronic F-127, Rhod-2 AM, Annexin V-Alexa 647 and Dihydrorhodamine 123 were from Invitrogen. L-(<sup>14</sup>C) valine was from Amersham, and the ImmunoCruz<sup>TM</sup> IP/WR Optima B system was supplied by Santa Cruz Biotechnology.

**Antibodies.** The antibodies were used as follows: p-eIF2 $\alpha$  (#9721), eIF2 $\alpha$  (#9722), p-PERK (#3179), caspase 3 (#9665) and Alix (#2171), Cell Signaling; 1/1000 diluted. GADD34 (sc-8327) and CHOP (sc-7351) Santa Cruz biotechnology; 1/1000 diluted. LC3b (PM036, MBL; 1/2000 diluted), ATF4 (ARP37017 Aviva Systems Biology; 1/10000 diluted), Xbp-1 (ab37152, Abcam, 1/1000 diluted). PERK (P0074, 1/1000 diluted) and  $\alpha$ -tubulin (1/8000 diluted) Sigma-Aldrich. Myc (05-724, Millipore, 1/1000 diluted), Lamp-1 (DSHB, 1/250 diluted), Mfn1 (kindly provided by Dr. Manuel Rojo, 1/200 diluted), Mfn2 (ab56889, Abcam, 1/1000 diluted), Opa1 (612606, BD Transduction, 1/1000 diluted), Drp1 (611112, BD Transduction, 1/1000 diluted), Fis1 (kindly provided by Dr. Yisang Yoon, 1/1000 diluted). Proteins were detected by the ECL method.

**Plasmids.** pAc-GFPC1-Sec61 $\beta$  (Plasmid #15108), p5xATF6-GL3 (Plasmid #11976), pBABE-puro mCherry-EGFP-LC3B (Plasmid #22418), pCL-Eco (Plasmid 12371) were from Addgene. mt-DsRED was from Clontech. BAK-GFP was a gift from Dr. Z. Dong (Department of Cellular Biology and Anatomy, Medical College of Georgia, USA). P8-HA-erRFP (ER-RFP) was a gift from Dr. F. Pimentel-Muinos (Centro de Investigacion del Cancer, Spain) (Klee & Pimentel-Muinos, 2005). Retroviral construct pBABE-PERK-myc was a gift from Dr. Alan Diehl (Abramson Family Cancer Research Institute, University of Pennsylvania, USA). pLenti-GIII-CMV-hMFN2-HA Lentiviral Vector was from Applied Biological Materials. pLKO.1-puro constructs for Mfn2 (TRCN0000080610), Mfn1 (TRCN0000081402), PERK (TRCN0000028831), XBP-1 (TRCN0000008420) and ATF6 (TRCN0000008449) were from Mission library (Sigma-Aldrich).

**Animal care and generation of animal models.** All animal work was done in compliance with guidelines established by the University of Barcelona's Committee on Animal Care. Mfn2<sup>loxP/loxP</sup> mice were provided by Dr. David Chan (Mfn2<sup>tm3Dcc</sup>/Mmcd) (Chen et al, 2007) through MMRRC. Homozygous Mfn2<sup>loxP/loxP</sup> mice were crossed either with a mouse strain expressing Cre recombinase under the control of the MEF2C promoter (mef2C-73k-Cre) (Heidt & Black, 2005) or with a mouse strain expressing Cre recombinase specifically in liver during neonatal life under the control of the albumin promoter (Alb-Cre) (The Jackson Laboratory, Bar Harbor, ME). Control and KO mice were littermates. Mice were kept under a 12-h dark-light period and were provided a standard chow-diet and water *ad libitum*.

**Western blotting assay.** Cells were homogenized in RIPA (150 mM NaCl, 10 mM Tris, pH 7.2, 0.1% SDS, 1% Triton X-100, 1% deoxycholate, 5 mM EDTA, 1 mM NaVO<sub>4</sub>, 5 mM NaF, 1 mM PMSF, and protease inhibitor mixture (Roche)) and centrifuged at 10000 x *g* for 15 min at 4°C. Tissue samples were homogenized in 10 volumes of RIPA buffer using a polytron. Homogenates were rotated for 1 h at 4°C in an orbital shaker and centrifuged at 10000 x *g* for 15 min at 4°C. Proteins from total homogenates were resolved in 10%, 12.5% or 15% acrylamide gels for SDS-PAGE and transferred to Immobilon membranes (Millipore).

**Transmission electron microscopy.** MEFs were washed twice with 0.1 M phosphate buffer at room temperature. For fixation, cells were incubated in 2.5% glutaraldehyde solution at room temperature for 70 min. Following post-fixation in 1% osmium tetroxide in 0.1 M phosphate buffer at 4°C for 2 h, cells were washed with highly pure water and kept overnight in 0.1 M phosphate buffer. Samples were then dehydrated at 4°C under shaking in graded solutions of acetone (50%, 70% and 90%) in highly pure water. Samples were gradually infiltrated with Eponate 12 Resin (TED PELLA 18010) and polymerization of the resin was performed for 48 h at 60°C. Thin sections (50-nm) were cut using a Leica EM UC6 (Leica, Vienna) and mounted on bare 200-mesh copper grids. Sections were stained with uranyl acetate 2% for 30 min, washed with highly pure water, and finally incubated for 5 min with lead citrate and air-dried. Sample sections were observed on an FEI CM-12 transmission electron microscope.

**Cell death assays.** Caspase 3 cleavage was determined in 50 µg RIPA total protein cell lysate of control and treated cells. DEVDase activity was determined in 30 µg of RIPA total protein cell lysate (without protease inhibitors). Cleavage of the fluorogenic

substrate Ac-DEVD-AFC (Bachem) was used to measure caspase activity. Fluorescence was quantified in a TECAN fluorometer. DNA fragmentation was determined in MEFs previously permeabilized with methanol and labeled with propidium iodide (PI). The sub-G1 population was quantified by flow cytometry. Necrosis was quantified by measuring lactate dehydrogenase (LDH) activity in cells and culture media using the LDH kit from Roche. The fraction of LDH released was determined by comparison of the LDH activity in culture medium relative to total LDH activity.

**Apoptosis assessment by Annexin V and PI staining.** WT and Mfn2 KO MEFs were harvested at the indicated times after treatment. Culture medium supernatant and PBS washes were retained to ensure that both floating and adherent cells were analyzed. After incubation for 15 min with Alexa 647-conjugated Annexin V (Invitrogen) following the manufacturer's instructions, cells were subjected to FACS analysis. PI was added 5 min prior to analysis.

**Autophagy flux analysis and protein degradation assay.** For the autophagic flux analysis, cells were incubated in the presence or absence of 100 nM bafilomycin for 4 h or for 6 h in the presence or absence of different stressors. After that time, they were processed for immunodetection of LC3b. LC3b-II abundance was normalized by tubulin levels, as described (Mauvezin et al, 2010).

To analyze the degradation of long-lived proteins, intracellular proteins were labeled for 24 h at 37°C by incubating cells at 50% of confluence with 0.2  $\mu$ Ci/ml L-[U-<sup>14</sup>C] valine (spec. activity 259mCi/mmol) in complete medium. Cells were then washed 3 times with PBS in order to eliminate the unincorporated radioactivity and then

incubated at 37°C for an additional hour with fresh complete medium with 10 mM L-valine to permit the degradation of short-lived proteins. Next, the medium was removed and cells were incubated in a range of experimental conditions in the presence of 10 mM L-valine for a further 4 h. After the treatment, the medium was collected and proteins were precipitated in TCA at a final concentration of 10%. The pellet was then dissolved in 200 µl of 0.2 N NaOH 0.4% Na-deoxycholate. Cells were washed twice with 10 mM L-valine in cold PBS, scrapped in 1 ml of PBS, and precipitated in TCA at a final concentration of 10%, and the pellet was dissolved as mentioned. The acid-soluble and also insoluble radioactivity from the medium, as well as the insoluble radioactivity from the cells, was measured by liquid scintillation counting (Mauvezin et al, 2010).

**Labeling of acidic compartment.** Cells were loaded with 100 nM LysoTracker Green (Molecular Probes, Invitrogene) for the last 20 min of incubation. Cells were then analyzed by flow cytometry.

**ER expansion studies.** Cells were treated with Tg 1 µM for 3 h and then loaded with 0.2 µg/ml Brefeldin A-BODIPY (Molecular Probes, Invitrogene) for 40 min, as reported (Hetz et al, 2006). Cells were then analyzed by flow cytometry.

**RNA extraction and Real-Time-PCR.** Total RNA extraction was performed with the RNeasy Mini Kit (Qiagen). RNA concentration was determined by spectrophotometry at an absorbance of 260 nm. RNA was reverse-transcribed with the SuperScript RT II

kit (Invitrogen). Real-time PCR was performed from 0.1 µg of total RNA from MEFs using specific primers (Supplementary Table 2). PCRs were performed using the StepOnePlus real-time PCR machine (Applied Biosystems) and ABI SYBR green reagents. All measurements were normalized to the housekeeping gene  $\beta$ -actin. UPR gene expression was assessed using a commercially 84 gene PCR array (RT<sup>2</sup> Profiler PCR Array system, SABiosciences).

## Supplementary Figures and Movie.

### Supplementary Figure 1. Mfn2 ablation promotes abnormal ER morphology upon

**ER stress.** (A) WT and Mfn2 KO cells were transfected with ER-RFP plasmid and then treated with 1  $\mu$ M Tg, 0.5  $\mu$ g/ml tunicamycin (Tm) or 100 ng/ml brefeldin (Bref) for 6 h. Cells were visualized for confocal microscopy. Scale bars: 10  $\mu$ m. (B) Immunodetection of HA epitope in Mfn2 KO cells stably expressing Mfn2-HA (Mfn2 KO + Mfn2) or an empty vector (Mfn2 KO group). (C) Representative confocal images of mitochondrial morphology stained with MitoTracker Green in Mfn2 KO cells stably expressing Mfn2-HA or an empty vector. Scale bars: 10  $\mu$ m. (D, E) Mfn2 KO cells or Mfn2 KO cells after re-expression of Mfn2 were transfected with ER-RFP plasmid (D) or with the Sec61 $\beta$ -GFP plasmid (E) and then treated with 1  $\mu$ M Tg for 24 h. Cells were visualized for confocal microscopy. Scale bars: 10  $\mu$ m.

### Supplementary Figure 2. Mfn2 knockdown promotes abnormal ER expansion

**during ER stress.** (A) Immunodetection of Mfn2 or Mfn1 in MEF cells stably expressing a shRNA (Scr), shRNAs directed against Mfn1 (Mfn1 KD) or Mfn2 (Mfn2 KD). (B) Representative confocal images of mitochondrial morphology stained with MitoTracker Green in MEF cells stably expressing a control shRNA (Scr), shRNAs directed against Mfn1 (Mfn1 KD) or Mfn2 (Mfn2 KD). Scale bars: 10  $\mu$ m. (C) WT, Mfn2 KD or Mfn1 KD MEFs were transfected with the Sec61 $\beta$ -GFP plasmid and treated with 1 $\mu$ M Tg for 24 h. Fluorescence microscopy images show ER vacuolization in Mfn2 KD cells treated with Tg. Scale bars: 10  $\mu$ m. Inset shows 10x zoomed images. Scale 5  $\mu$ m.

**Supplementary Figure 3. Mfn2 ablation reduces apoptosis upon ER stress.** (A) Basal caspase activity in WT and Mfn2 KO MEF cells, Scr, in Mfn2 KD 3T3-L1 fibroblasts and in Scr and Mfn2 KD C2C12 myoblasts was assessed by measuring the cleavage of the fluorogenic substrate DEVD-AFC. (B) Apoptosis detection in Mfn2 KO cells and Mfn2 KO cells stably expressing Mfn2-HA treated with 1  $\mu$ M Tg for 24 h. Total and cleaved caspase 3 levels were detected by Western blot. (C, D) Apoptosis detection in WT, Mfn1 KO and Mfn2 KO cells treated with 1  $\mu$ M Tg, 0.5  $\mu$ g/ml tunicamycin (Tm) or 100 ng/ml Brefeldin A (Bref) for 24 h. Total and cleaved caspase 3 levels were detected by Western blot (C) and caspase activity (D) by measurement of DEVD-AFC substrate processing. Data are given as mean  $\pm$  SEM. \*,  $p < 0.05$  vs. WT groups; #,  $p < 0.05$  vs. Mfn1 KO groups. (E) WT and Mfn2 KO cells were incubated with 30 ng/ml TNF $\alpha$  in the presence or absence of CHX (10  $\mu$ M) and z-VAD-fmk (20  $\mu$ M) for 4 h, in the presence or absence of 1  $\mu$ M staurosporine (STS) for 6 h or 1  $\mu$ M Tg for 24 h. Total and cleaved caspase 3 levels were detected by Western blot. (F) WT and Mfn2 KD C2C12 myoblasts were treated with 1  $\mu$ M Tg for 12 or 16 h, and total and cleaved caspase 3 levels were detected by Western blot. Data are given as mean  $\pm$  SEM. \*,  $p < 0.05$  vs. WT non-Tg-treated group. (G) WT and Mfn2 KO cells were incubated with 1  $\mu$ M Tg for 16 h in the presence or absence of 100 nM CHX and stained with Annexin V/PI for flow cytometry measurements. Data are given as mean  $\pm$  SEM. \*,  $p < 0.05$  vs. Mfn2 KO+Tg group.

**Supplementary Figure 4. Mitochondrial morphology in 3T3-L1 fibroblasts and C2C12 myoblasts upon Mfn2 loss-of-function.** (A,C) Mfn2 immunodetection in Scr



and Mfn2 KD 3T3-L1 fibroblasts and Scr and Mfn2 KD C2C12 myoblasts. Tubulin was used as loading control. **(B,D)** Cells were transfected with mt-DsRed plasmid and mitochondrial morphology was visualized by confocal microscopy. Scale bars: 10  $\mu$ m.

**Supplementary Figure 5. Mfn2 knockdown reduces ER stress-induced autophagy.**

**(A)** LC3-I and LC3-II abundance in Mfn2 KO cells upon stable re-expression of Mfn2. Cells were treated or not with 1  $\mu$ M Tg for 24 h. **(B, C, D)** WT or Mfn1 KO cells were treated with 1  $\mu$ M Tg for a range of times **(B, C)** or for 6 or 12 h in the presence or absence of bafilomycin (Baf, 100 nM) **(D)**. LC3-I and LC3-II abundance was determined by immunodetection. Data are given as mean  $\pm$  SEM. **(E)** Acidic compartments of WT or Mfn1 KO cells were stained with LysoTracker Green and analyzed by flow cytometry. Data are given as mean  $\pm$  SEM. \*,  $p < 0.05$  vs. WT group. **(F, G)** 3T3-L1 fibroblasts or C2C12 myoblasts stably expressing a scrambled shRNA (Scr) or a shRNA directed against Mfn2 (Mfn2 KD) were treated as indicated (1  $\mu$ M Tg, 100 nM Baf) for 6 h. Autophagy flux was assessed in Baf-treated cells by LC3b II immunodetection. **(H)** Degradation assays for long-lived protein in Scr and Mfn2 KD 3T3-L1 fibroblasts treated with 0.5  $\mu$ g/ml Tm for 16 h. Data are given as mean  $\pm$  SEM. \*,  $p < 0.05$  vs. Scr group.

**Supplementary Figure 6. ATF6 knockdown potentiates ER expansion and cell**

**death in Mfn2-ablated cells.** **(A)** ATF6 transcriptional activity in Mfn2 KO cells that stably express scramble (Scr) or shRNA directed against ATF6. Cells were transfected with 5xATF6-GL3 and TK-*Renilla* plasmids and then treated with 1  $\mu$ M Tg for 24 h. Data are mean  $\pm$  SEM. \*,  $p < 0.05$  vs. basal; #,  $p < 0.05$  vs. Scr group. **(B)** ER expansion

was assessed in Scr or ATF6 shRNA Mfn2 KO cells treated with Tg. Cells were transfected with Sec61 $\beta$ -GFP and treated with 1 $\mu$ M Tg for 6 h. Scale bars: 10  $\mu$ m. **(C)** Scr or ATF6 shRNA WT and Mfn2 KO cells were treated with 1  $\mu$ M Tg with and without 100 nM Bafilomycin for 6 h. Autophagy flux was assessed by LC3b-II immunodetection. **(D)** Viability of Scr or ATF6 shRNA Mfn2 KO cells treated with 1  $\mu$ M Tg for 24 h was assessed using the PI permeability method. Data are mean  $\pm$  SEM. \* $p$ <0.05 vs. Scr group. **(E and F)** Apoptosis detection in Scr or ATF6 shRNA WT and Mfn2 KO cells treated with Tg for 24 h. Caspase activity was assayed by measurement of DEVD-AFC substrate processing **(E)**. Total and cleaved caspase 3 levels were detected by Western blot **(F)**. Data are mean  $\pm$  SEM. \* $p$ <0.05 vs. WT groups.

**Supplementary Figure 7. Mitochondrial morphology and function in Mfn2 KO cells.** **(A)** Representative confocal images of mitochondrial morphology in WT and Mfn2 KO cells stained with MitoTracker Red CMXRos. Scale bars: 10  $\mu$ m. **(B)** Mitochondrial swelling of Mfn2 KO cells. Representative confocal images of mitochondria in WT and Mfn2 KO cells previously transfected with the BAK-GFP plasmid. Scale bars: 10  $\mu$ m. **(C)** Flow cytometry quantification of ROS levels in WT and Mfn2 KO cells using DHR 1,2,3. Data are mean  $\pm$  SEM. \* $p$ <0.05 vs. WT. **(D)** Quantification of the mitochondrial oxygen consumption rate (OCR) in WT and Mfn2 KO cells. Non-mitochondrial OCR was determined by the addition of the complex III inhibitor antimycin A (0.1  $\mu$ M) and subtracted from the total OCR in order to obtain mitochondrial OCR. Data are mean  $\pm$  SEM. \* $p$ <0.05 vs. WT. **(E)** Mitochondrial calcium overload in WT and Mfn2 KO cells. *(left)* Cells were loaded with Rhod-2 and then treated with CaCl<sub>2</sub> 2.5 mM. Calcium uptake was monitored by confocal

microscopy. (*right*) Representative confocal images of mitochondrial morphology in WT and Mfn2 KO cells stained with Rhod-2 and incubated with 2.5mM CaCl<sub>2</sub> for 5 min. Scale bars: 10  $\mu$ m. (*F*) Flow cytometry quantification of ROS levels (measured by using DHR 1,2,3) in Mfn2 KO cells stably expressing Mfn2-HA (Mfn2 KO + Mfn2) or an empty vector (Mfn2 KO group). Data are mean  $\pm$  SEM. \*p<0.05 vs. Mfn2 KO group. (*G*) Quantification of the mitochondrial OCR in Mfn2 KO cells stably expressing Mfn2-HA (Mfn2 KO + Mfn2) or an empty vector (Mfn2 KO group). Data are mean  $\pm$  SEM. \*p<0.05 vs. Mfn2 KO group.

**Supplementary Figure 8. Effect of PERK XBP-1, ATF6 knockdown in Mfn2 KO cells.** (*A*) Representative confocal images of mitochondrial morphology stained with MitoTracker Green in WT and Mfn2 KO cells stably expressing a scrambled shRNA (Scr) or a shRNA directed against XBP-1 (XBP-1 KD) or against ATF6 (ATF6 KD). Scale bars: 10  $\mu$ m. (*B, and C*) Immunodetection of Mfn1, Drp1, Fis1 and Opa1 in WT and Mfn2 KO cells stably expressing a scrambled shRNA (Scr) or a shRNA directed against PERK (PERK KD).

## **Movies**

**Movie 1.** ER vacuolization of Mfn2 KO cells. Mfn2 KO cells were transfected with ER-RFP, and ER vacuolization was observed by live cell imaging. Time series of ER vacuolization were collected every 5 min.

Supplementary Table 1. Effect of Mfn2 ablation on UPR target gene expression

Symbol	WT + Tg		Mfn2 KO		Mfn2 KO + Tg		
	mean	SEM	mean	SEM	mean	SEM	t-student
Ddit3	9.32	1.44	5.90	2.79	31.08	5.78	*
Herpud1	8.48	0.15	4.37	3.36	22.82	1.78	*
Hspa5	7.69	0.20	4.02	3.00	16.44	1.36	*
Atf4	5.59	0.28	3.04	2.09	12.30	1.42	*
Serp1	4.15	0.16	2.21	1.58	10.96	0.81	*
Manf	5.36	0.33	2.96	1.96	10.71	1.43	*
Atf6	4.70	0.77	3.02	1.38	8.55	3.90	
Ero1l	6.48	0.86	3.98	2.04	8.42	0.95	*
Edem1	3.40	0.71	2.31	0.88	6.74	1.59	*
Ero1lb	3.26	0.28	1.87	1.13	6.69	0.42	*
Xbp1	4.59	0.52	2.75	1.50	6.52	0.11	*
Syvn1	2.66	0.35	1.63	0.84	6.01	0.31	*
Dnajc3	2.43	0.38	1.54	0.73	5.45	0.82	*
Sel1l	3.65	0.54	2.29	1.11	4.37	1.44	
Rpn1	1.53	0.12	0.86	0.54	4.20	0.14	*
Dnajb9	2.39	0.11	1.29	0.89	4.19	0.31	*
Sec63	2.73	1.78	2.90	0.15	3.93	2.47	
Calr	2.14	0.76	1.73	0.34	3.84	1.63	
Pdia3	2.12	0.08	1.13	0.81	3.71	0.20	*
Ufd1l	1.84	0.21	1.10	0.60	3.26	0.36	*
Htra2	1.63	0.02	0.84	0.65	3.09	0.02	*
Canx	1.88	0.39	1.28	0.50	3.07	0.94	*
Edem3	1.46	0.26	0.95	0.42	2.92	0.42	*
Derl2	1.94	0.24	1.18	0.62	2.86	0.34	
Cct7	2.35	1.18	2.20	0.12	2.80	0.22	
Cct4	2.05	0.08	1.10	0.78	2.78	0.49	
Ube2j2	1.34	0.10	0.76	0.48	2.62	0.20	*
Bax	1.70	0.10	0.94	0.63	2.37	0.48	
Ubxn4	1.21	0.07	0.67	0.44	2.33	0.31	
Derl1	1.35	0.34	0.97	0.31	2.29	0.78	
Tcp1	1.50	0.16	0.88	0.50	2.15	0.26	
Dnajb2	1.52	0.07	0.82	0.57	2.13	0.46	
Usp14	1.67	0.26	1.06	0.49	1.80	0.22	
Atf6b	1.32	0.11	0.76	0.46	1.79	0.26	
Mbtps2	2.06	0.16	1.17	0.73	1.68	0.16	
Ube2g2	1.98	0.03	1.01	0.79	1.62	0.04	*
Insig2	1.64	0.06	0.87	0.63	1.41	0.15	
Ern2	1.50	0.62	1.29	0.17	1.32	0.43	

Mean±SEM of 3 independent experiments.

Data are expressed relative to untreated wild type cells.

## Supplementary Table 2

### Real Time-PCR

beta-actin

Fw: GGTCATCACTATTGGCAACGA

Rv: GTCAGCAATGCCTGGGTACA

Beclin-1

Fw: TCGATTTTGTCTTCCGTACAGGA

Rv: GCATGAACTTGAGCGCTTTTG

LC3b

Fw: AGCTCTTTGTTGGTGTGTAAGTGTCT

Rev: TTGTCCTCACAGCTGACATGTATG

## References.

Chen H, McCaffery JM, Chan DC (2007) Mitochondrial fusion protects against neurodegeneration in the cerebellum. *Cell* **130**: 548-562

Heidt AB, Black BL (2005) Transgenic mice that express Cre recombinase under control of a skeletal muscle-specific promoter from *mef2c*. *Genesis* **42**: 28-32

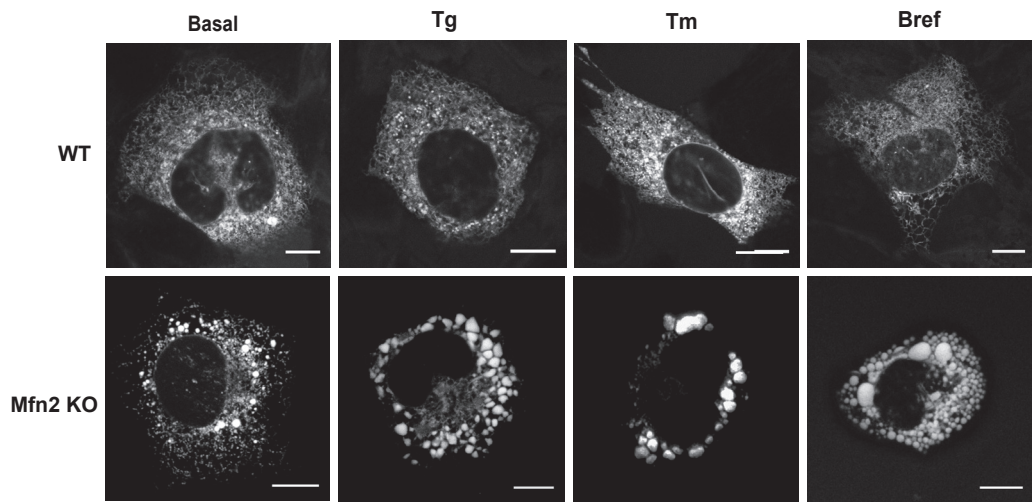
Hetz C, Bernasconi P, Fisher J, Lee AH, Bassik MC, Antonsson B, Brandt GS, Iwakoshi NN, Schinzel A, Glimcher LH, Korsmeyer SJ (2006) Proapoptotic BAX and BAK modulate the unfolded protein response by a direct interaction with IRE1alpha. *Science* **312**: 572-576

Klee M, Pimentel-Muinos FX (2005) Bcl-X(L) specifically activates Bak to induce swelling and restructuring of the endoplasmic reticulum. *The Journal of cell biology* **168**: 723-734

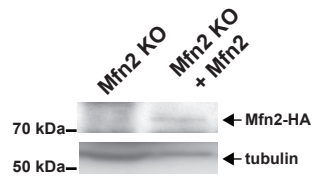
Mauvezin C, Orpinell M, Francis VA, Mansilla F, Duran J, Ribas V, Palacin M, Boya P, Telemann AA, Zorzano A (2010) The nuclear cofactor DOR regulates autophagy in mammalian and *Drosophila* cells. *EMBO reports* **11**: 37-44

# Supplementary Fig 1

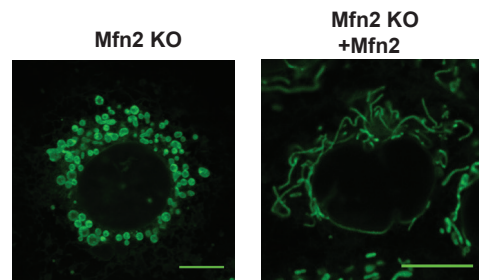
**A**



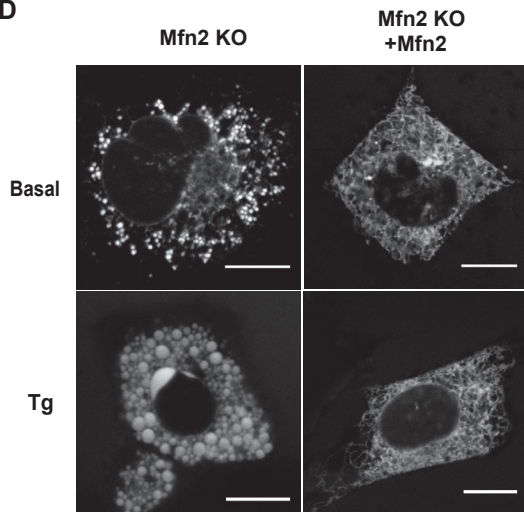
**B**



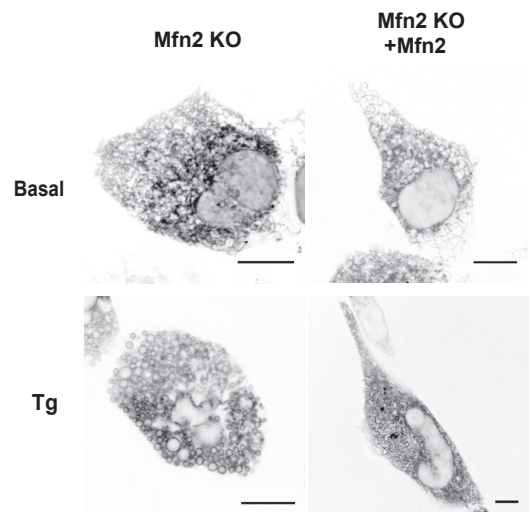
**C**



**D**

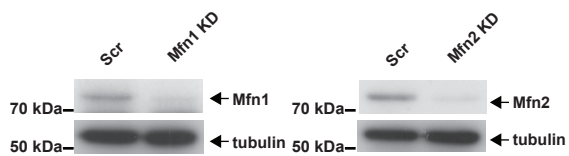


**E**

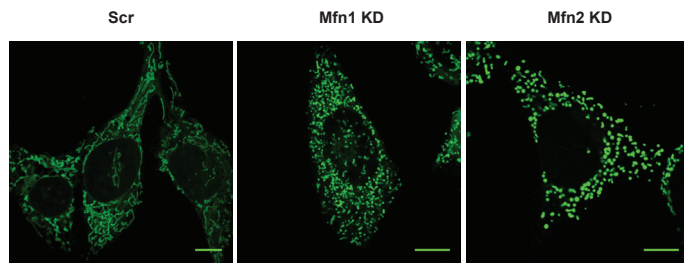


# Supplementary Fig 2

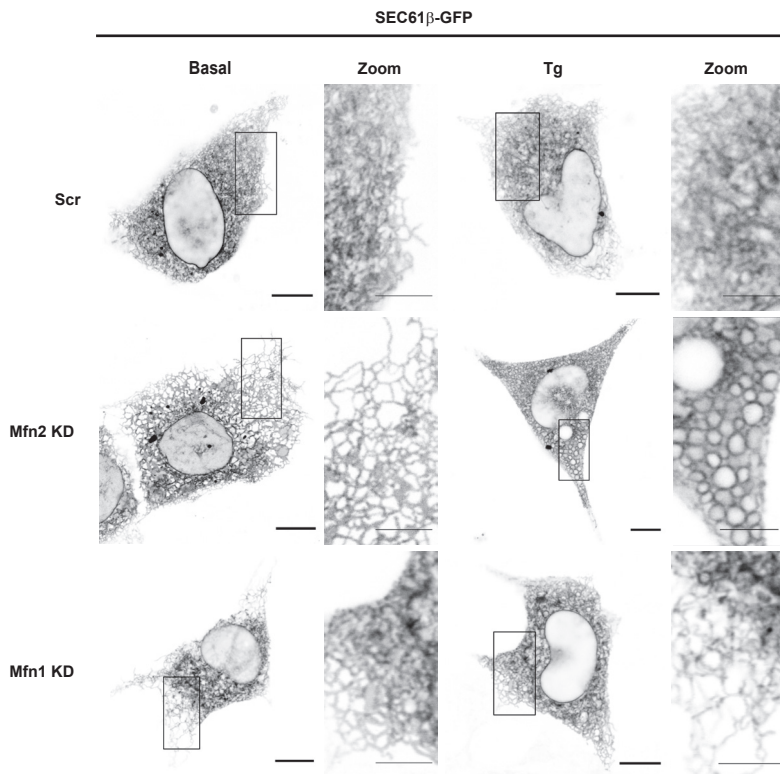
## A



## B

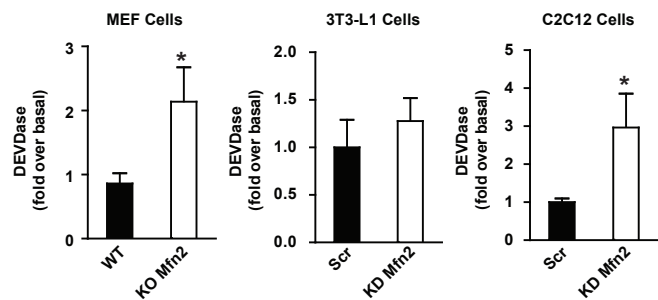


## C

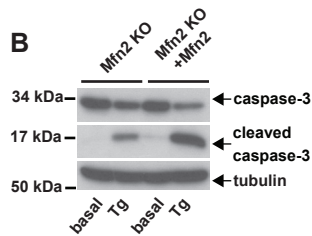




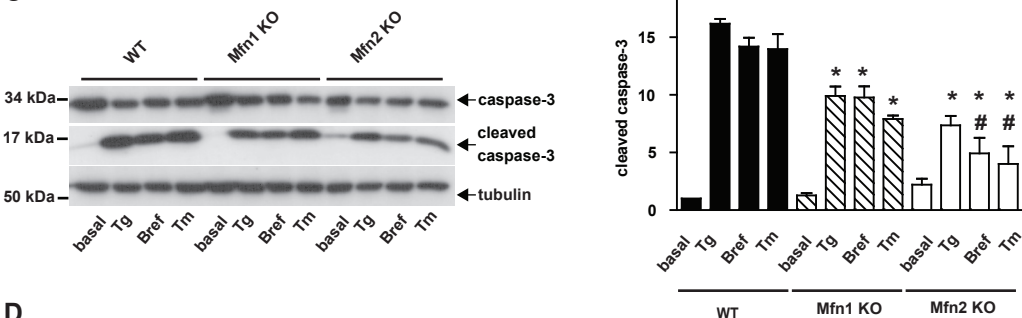
**A**



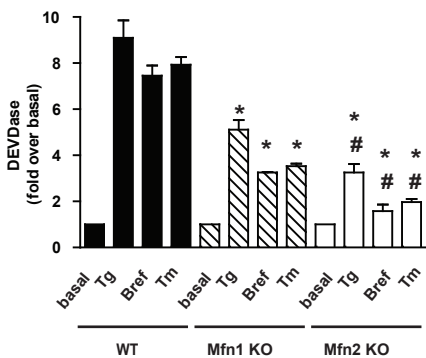
**B**



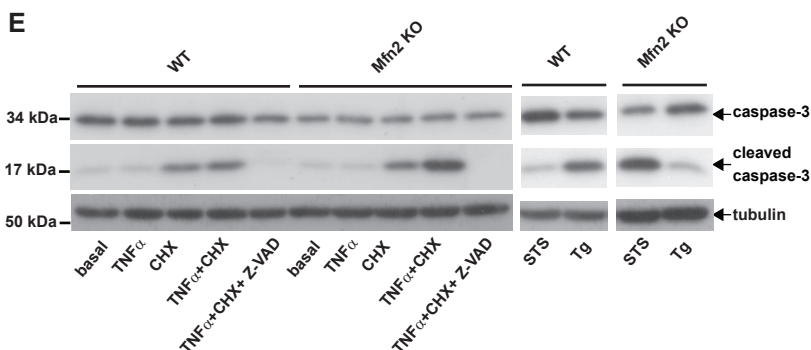
**C**



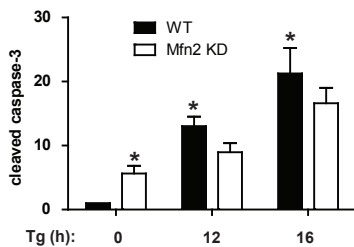
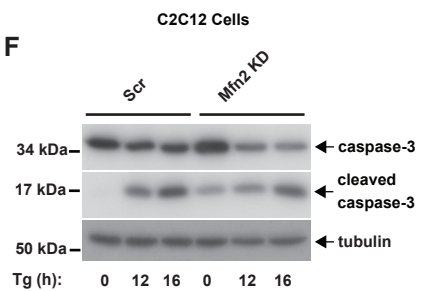
**D**



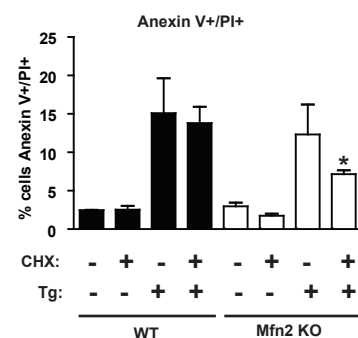
**E**



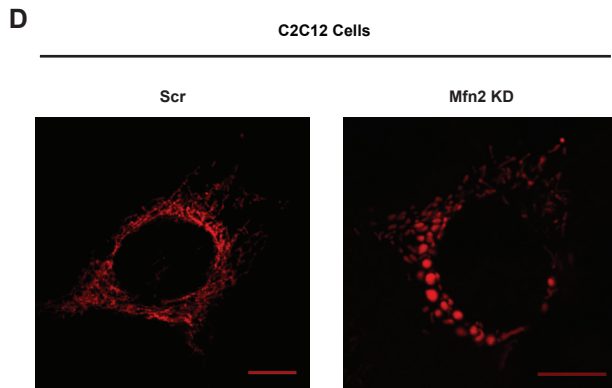
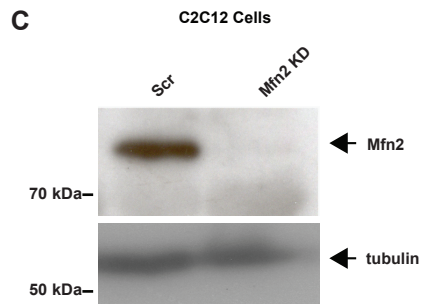
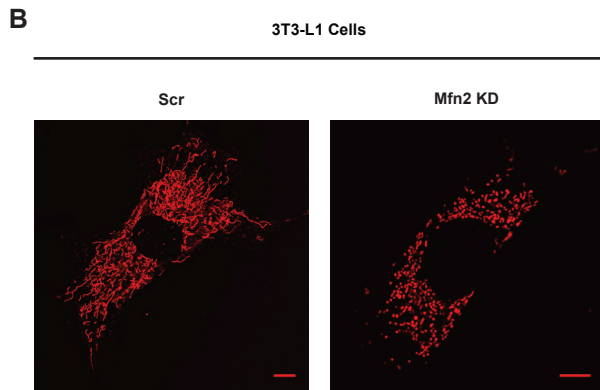
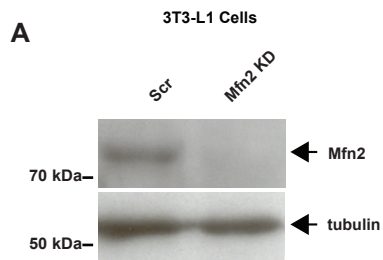
**F**



**G**

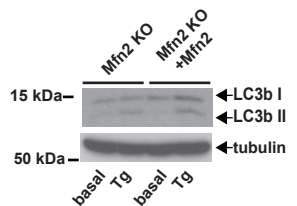


## Supplementary Fig 4

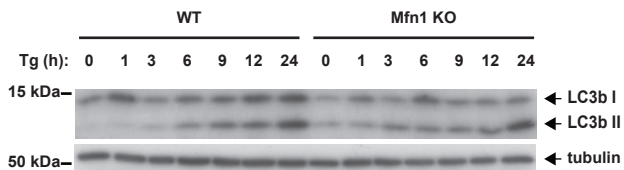


# Supplementary Fig 5

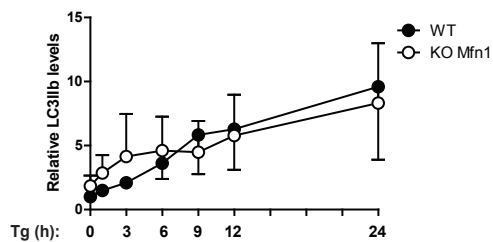
## A



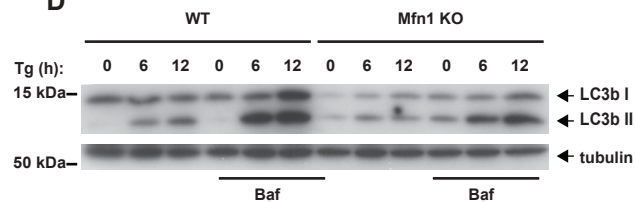
## B



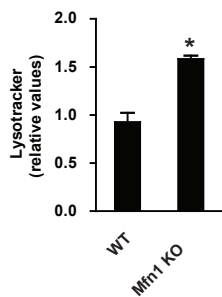
## C



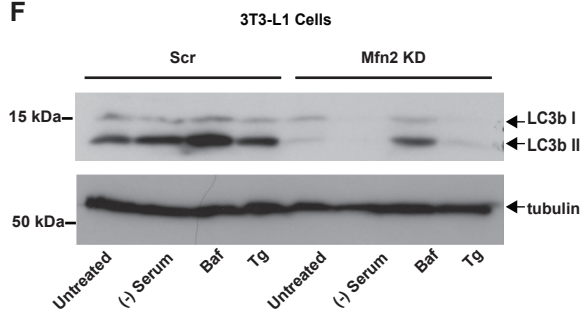
## D



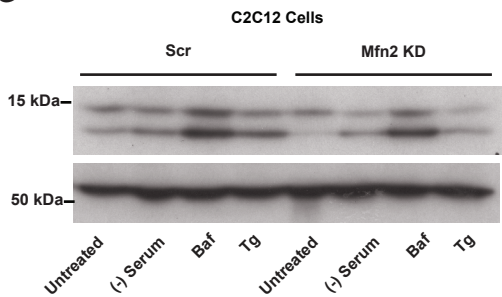
## E



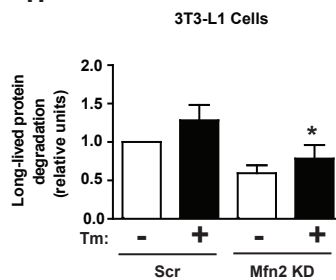
## F



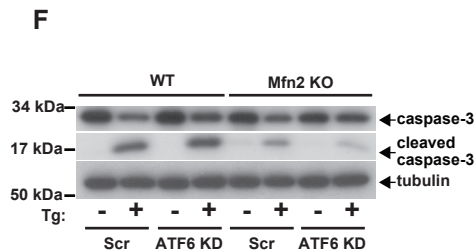
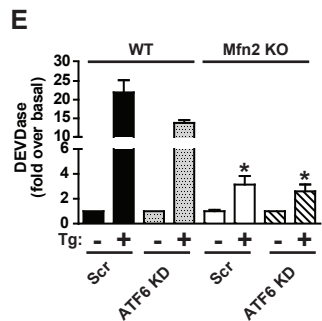
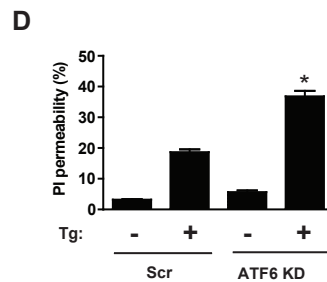
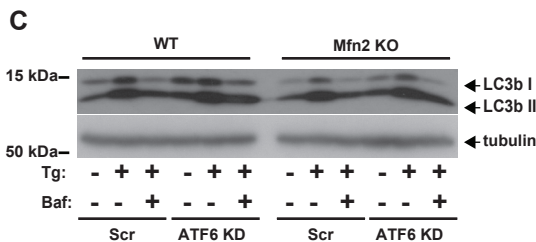
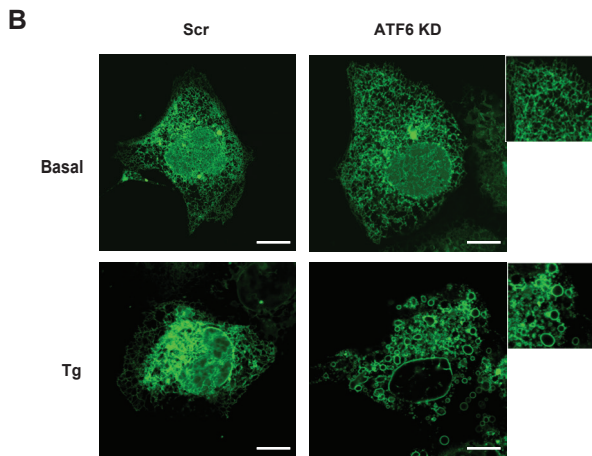
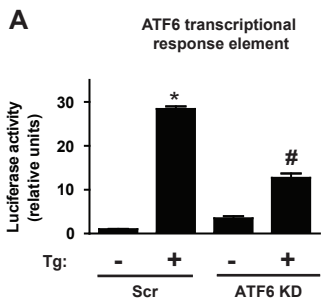
## G



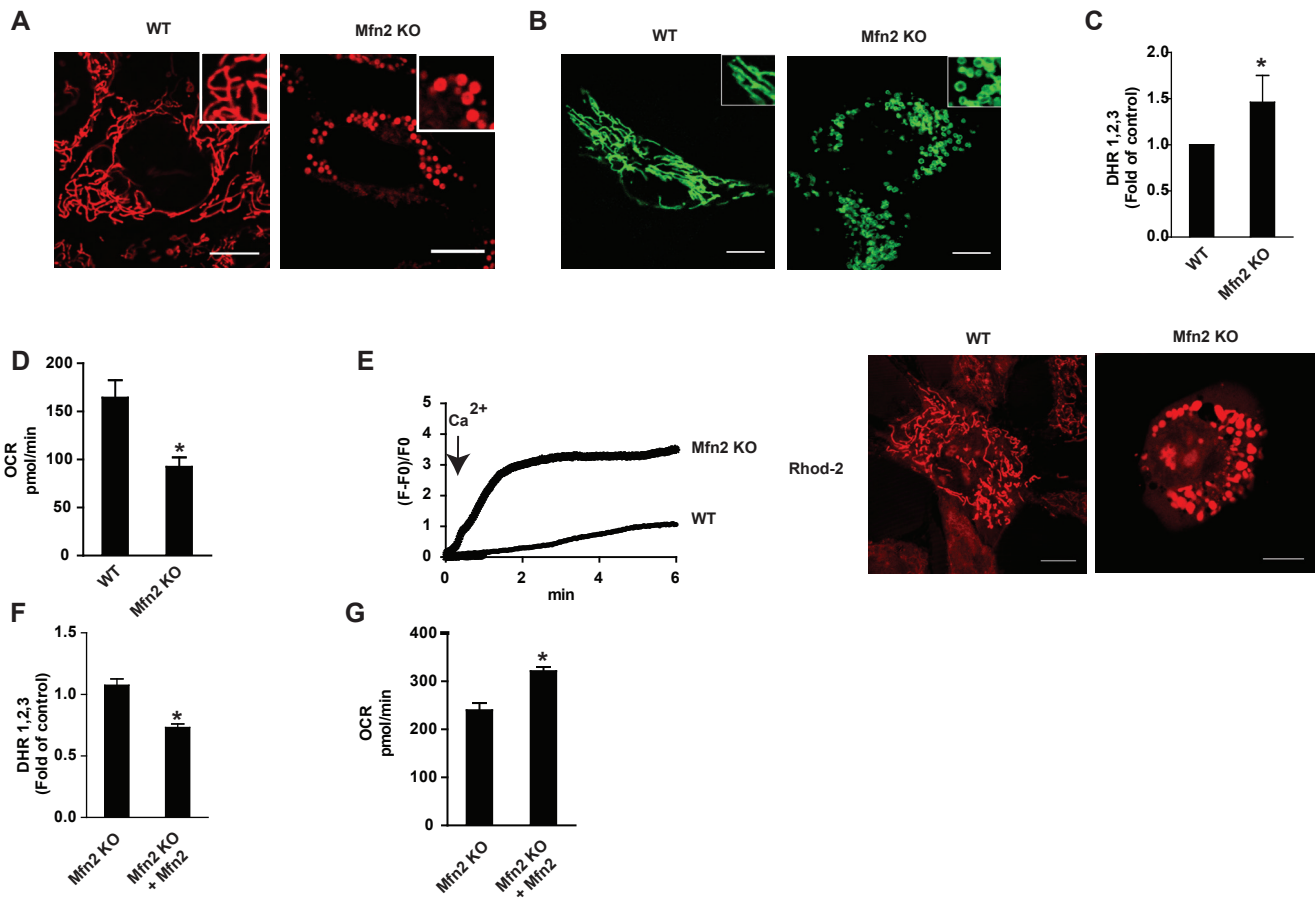
## H



# Supplementary Fig 6



# Supplementary Fig 7



# Supplementary Fig 8

